JOC The Journal of Organic Chemistry

Article

pubs.acs.org/joc

Metal-Free Synthesis of 3-Arylquinolin-2-ones from Acrylic Amides via a Highly Regioselective 1,2-Aryl Migration: An Experimental and Computational Study

Le Liu,[†,§] Tonghuan Zhang,[‡,§] Yun-Fang Yang,[‡] Daisy Zhang-Negrerie,[†] Xinhao Zhang,[‡] Yunfei Du,[*,†] Yun-Dong Wu,[*,‡] and Kang Zhao[*,†]

[†]Tianjin Key Laboratory for Modern Drug Delivery & High-Efficiency, School of Pharmaceutical Science and Technology, Tianjin University, Tianjin 300072, China

[‡]Lab of Computational Chemistry and Drug Design, Key Laboratory of Chemical Genomics, Peking University Shenzhen Graduate School, Shenzhen 518055, China

Supporting Information

ABSTRACT: Combined experimental and theoretical investigations into the phenyliodine bis(trifluoroacetate) (PIFA)-mediated reaction of *N*-arylcinnamamide to produce 3-arylquinolin-2-one derivatives have been conducted. High regioselectivity during the aryl migration process was observed in 3,3-disubstituted acrylamides. Density functional theory calculation was conducted in an attempt to understand the mechanism and the origin of the regioselectivity. On the basis of both the experimental and the theoretical results, a mechanism involving an oxidative annulation, followed by an aryl migration, has been proposed. The annulation is the regioselectivity determining step.

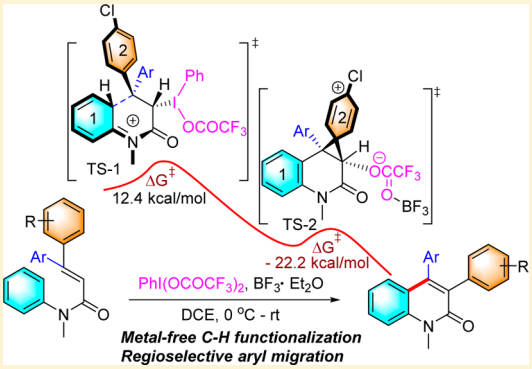

INTRODUCTION

C−H functionalization, having emerged over the past few decades, represents an attractive area of great significance for its capacity to directly enhance molecular complexity.[1] Numerous elegant works have been reported in recent decades on the construction of heterocyclic compounds via C−H functionalization.[2] The frameworks of quinolin-2-one compounds, especially those bearing 3-aryl groups, are frequently found in many natural products and pharmaceutically active molecules, examples of which are shown in Figure 1.[3] Compounds with the 3-arylquinolin-2-one subunit have been used as anticancer,[4a] antiplatelet,[4b] and antihypertensive agents.[4c] Moreover, they are also valuable building blocks for the synthesis of many natural alkaloids.[5] Therefore, many efforts for the synthesis and functionalization of this class of molecules have been made. Aside from the classic base-catalyzed Friedländer reaction[5] and the acid-catalyzed Knorr synthesis,[6] several alternative approaches have been disclosed for accessing quinolin-2-one skeletons based on C−H activation including metal-catalyzed intra-[7a] or intermolecular[7b] carbocyclization of internal alkynes, Pd-catalyzed amidation of *o*-carbonyl-substituted aryl halides,[7c] and tandem decarboxylative radical addition/cyclization of *N*-arylcinnamaides with aliphatic carboxylic acids.[7d] Recently, Jiao and co-workers reported a synthesis of quinolin-2-ones involving an efficient Rh-catalyzed carbonylation and annulation of simple CO-containing anilines and alkynes through N−H and C−H bond activation.[7e] In addition, Dong and co-workers reported a Rh-catalyzed [5 + 2 − 1] transformation between isatins and alkynes to synthesize 2-quinolinone derivatives, proposed to proceed through an exclusive C−C activation, decarbonylation, and alkyne insertion process.[7f] All the aforementioned methods have merit in the preparation of the corresponding quinolin-2-ones, but a majority of these methods suffer one or more limitations such as harsh reaction conditions, involvement of transition metals, and limited substrate scope. Compared with the intensively investigated transition-metal-catalyzed processes, metal-free methods are less explored.[8] Therefore, the development of alternative mild and metal-free procedures involving C−H functionalization for the construction of quinolinones remains of great significance.

Hypervalent iodine reagents, featuring readily available, low toxicity, and environmentally benign properties, have fascinated chemists for a couple of decades. Consequently, a handful of efficient organic transformations mediated by hypervalent iodine reagents have been reported.[9] As a continuation of our work on hypervalent chemistry,[10] we extended our research on the metal-free approach to construct the 3-arylquinolinone skeleton from the readily available *N*-arylcinnamamides by focusing on the intriguing stereoselectivity and the mechanistic studies. Some initial results concerning the construction of core

Received: February 17, 2016
Published: April 28, 2016

ACS Publications © 2016 American Chemical Society

DOI: 10.1021/acs.joc.6b00345
J. Org. Chem. 2016, 81, 4058−4065

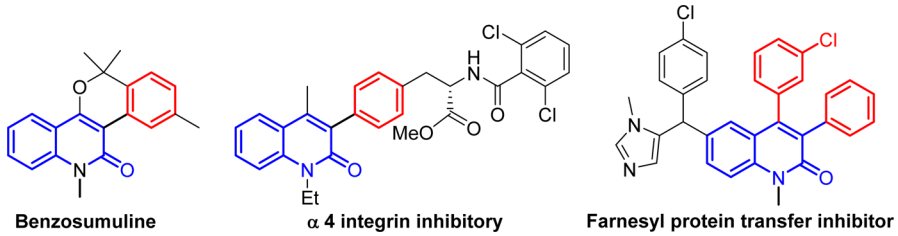

Figure 1. Representative biological or natural compounds bearing a 3-arylquinolin-2-one framework.

Table 1. Optimization for the Synthesis of Quinolinones Mediated by I(III)[a]

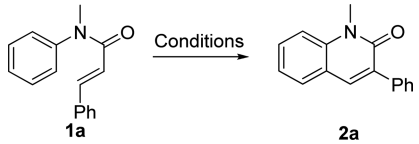

entry	solvent	oxidant (equiv)	additive (equiv)	time (h)	yield (%)[b]
1	DCE	PIFA (1.5)	$BF_3{\cdot}Et_2O$ (1)	12	20
2	DCE	PIFA (1.5)		24	NR
3	THF	PIFA (1.5)	$BF_3{\cdot}Et_2O$ (1)	12	trace
4	EA	PIFA (1.5)	$BF_3{\cdot}Et_2O$ (1)	10	15
5	CH_3CN	PIFA (1.5)	$BF_3{\cdot}Et_2O$ (1)	12	17
6	MeOH	PIFA (1.5)	$BF_3{\cdot}Et_2O$ (1)	24	NR
7	CF_3CH_2OH	PIFA (1.5)	$BF_3{\cdot}Et_2O$ (1)	12	20
8	DMF	PIFA (1.5)	$BF_3{\cdot}Et_2O$ (1)	24	NR
9	DCE	PIFA (1.5)	TFA (5)	24	43
10	DCE	PIFA (1.5)	$BF_3{\cdot}Et_2O$ (1)/TFA (5)	12	60
11	DCE	PIFA (1.5)	$BF_3{\cdot}Et_2O$ (1)/TFA (10)	6	68
12	DCE	PIFA (1.5)	$BF_3{\cdot}Et_2O$ (1)/TFA (20)	6	67
13[c]	DCE	PIFA (1.5)	$BF_3{\cdot}Et_2O$ (1)/TFA (10)	6	72
14[d]	DCE	PIFA (1.5)	$BF_3{\cdot}Et_2O$ (1)/TFA (10)	6	88
15[e]	DCE	PIFA (1.5)	$BF_3{\cdot}Et_2O$ (1)/TFA (10)	6	85
16[d,f]	DCE	PIFA (1.0)	$BF_3{\cdot}Et_2O$ (1)/TFA (10)	24	70
17[d]	DCE	PIFA (2.0)	$BF_3{\cdot}Et_2O$ (1)/TFA (10)	8	85
18[d]	DCE	PIDA (2.0)	$BF_3{\cdot}Et_2O$ (1)/TFA (10)	6	65
19[d]	DCE	PhIO (2.0)	$BF_3{\cdot}Et_2O$ (1)/TFA (10)	12	ND
20[d]	DCE	IBX (2.0)	$BF_3{\cdot}Et_2O$ (1)/TFA (10)	12	ND

[a]All the reactions were carried out at rt with **1a** (0.4 mmol) at the concentration of 0.1 M. [b]Isolated yield. [c]The concentration of **1a** was reduced to 0.05 M. [d]The concentration of **1a** was 0.025 M. [e]The concentration of **1a** was 0.01 M. [f]Based on 80% conversion of **1a**. NR = no reaction. ND = no desired product.

skeleton have been reported in an early communication.[11] In this paper, we present the evidence for a mechanism consisting of an exclusive I(III)-mediated oxidative C(sp^2)−C(sp^2) bond formation, followed by a 1,2-aryl migration,[12] with extremely high regioselectivity supported by both experimental observations and theoretical investigations of the transition-state structures and reaction coordinate energy profiles.

RESULTS AND DISCUSSION

N-Arylacrylamide derivatives, which have been well studied and used as useful substrates for the construction of heterocyclic frameworks through oxidative C−C bond formation,[13] were selected as model substrates. To our delight, the reaction of 1.0 equiv of **1a** with 1.5 equiv of PIFA in the presence of 1.0 equiv of $BF_3{\cdot}Et_2O$ in DCE afforded a 20% yield of a six-membered *N*-methyl-3-phenylquinolin-2(1*H*)-one **2a** (Table 1, entry 1). The reaction appeared to involve an unprecedented oxidative C−C bond formation and a 1,2-aryl migration. Further studies were subsequently carried out to formulate the optimal conditions for the transformation. As shown in Table 1, the substrate turned out to be inert to treatment with the oxidant PIFA in the absence of Lewis acid ($BF_3{\cdot}Et_2O$) (Table 1, entry 2). Solvent-screening tests of THF, CH_3CN, MeOH, TFE, and DMF showed that none of them are more effective than DCE for the desired reaction (Table 1, entries 2−8). An increased yield was observed when the additive was switched to TFA. The desired product was isolated in a much improved yield of 43% (Table 1, entry 9). When $BF_3{\cdot}Et_2O$ and TFA were combined and used as coadditive, the yield was improved to 60% (Table 1, entry 10). With an increased dosage of TFA, the yield continued to improve to 68% and the reaction time was dramatically shortened to 6 h (Table 1, entry 11). However, further increase of the dosage beyond 10 equiv provided no further improvement in the yield (Table 1, entry 12). Concentration screening with the starting substrate indicated that dilution favors the reaction, with the most ideal concentration identified to be 0.025 M (Table 1. entries 12−15). Evaluation of the most appropriate amount of the oxidant found the optimal amount of PIFA to be 1.5 equiv (Table 1, entries 16 and 17). Applications of other hypervalent iodine

DOI: 10.1021/acs.joc.6b00345
J. Org. Chem. 2016, 81, 4058−4065

Table 2. Synthesis of 3-Arylquinolin-2-one via PIFA-Mediated C−C Bond Formation and 1,2-Aryl Migration

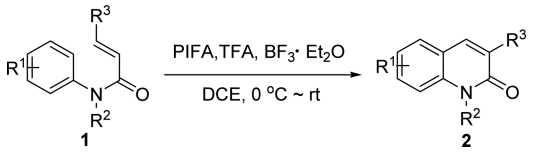

	substrate **1**						
entry[a]	R^1	R^2	R^3		**2**	time (h)	yield (%)[b]
1	H	Me	Ph	**1a**	**2a**	6	88
2	H	Bn	Ph	**1b**	**2b**	6	75
3	H	*i*-Pr	Ph	**1c**	**2c**	6	90
4	H	cPrMe	Ph	**1d**	**2d**	7	71
5	H	H	Ph	**1e**	**2e**	12	0
6	4-Me	Me	Ph	**1f**	**2f**	6	55
7	4-MeO	Me	Ph	**1g**	**2g**	5	48
8	4-Br	Me	Ph	**1h**	**2h**	7	87
9	3-F	Me	Ph	**1i**	**2i**/**2i′**	8	50[c]
10	3-CF_3	Me	Ph	**1j**	**2j**/**2j′**	6	77[d]
11	2-Cl	Me	Ph	**1k**	**2k**	7	78
12	2-CO_2Me	Me	Ph	**1l**	**2l**	7	44
13	H	Me	4-MeO-Ph	**1m**	**2m**	10	63[e]
14	H	Me	4-Br-Ph	**1n**	**2n**	12	34
15	H	Me	2-Cl-Ph	**1o**	**2o**	12	41
16	H	Me	2-Br-Ph	**1q**	**2q**	12	44
17	H	Me	2-thienyl	**1r**	**2r**	6	30
18	H	Me	Me	**1s**	**2s**	12	0

[a]All reactions were carried out with **1a** (0.4 mmol) and PIFA (1.5 equiv) in DCE (16 mL) unless otherwise stated. [b]Isolated yield. [c]The ratio of **2i** (7-F) and **2i′** (5-F) is 1.2:1. [d]The ratio of **2j** (7-CF_3) and **2j′** (5-CF_3) is 1.3:1. [e]TFA was used as the solvent. cPrMe = cyclopropylmethyl.

reagents including PIDA, PhIO, and IBX resulted in a decreased yield or no desired product. Combining all the testing results, the optimized conditions are determined to be 0.025 M of reactant, 1.5 equiv of PIFA as oxidant, and a combination of 1 equiv of BF_3·Et_2O and 10 equiv of TFA as coadditives in DCE as solvent (Table 1, entry 14).

Under the optimal reaction conditions, the scope and generality of this method were explored. The results, summarized in Table 2, show that substrates bearing benzyl (**1b**), isopropyl (**1c**), and cyclopropylmethyl (**1d**) substituents on the nitrogen atom were all transformed to the desired cyclized/migrated products in good to excellent yields (Table 2, entries 2−4). However, for the cinnamamide that bears no substitution on the nitrogen atom, the reaction resulted in a complex mixture, without any trace of the desired product (Table 2, entry 5). On a side note, we did find that debenzylation of **2b** with NBS in the presence of AIBN under reflux in chlorobenzene proceeded smoothly to give the NH product **2e** in 83% yield.[11]

As for the R^2 group, both electron-donating and electron-withdrawing groups at the *para*-position were well tolerated (Table 2, entries 6−8), albeit the electron-rich amide **1g** was converted to **2g** in a slightly lower yield. In the cases of substrates bearing either a F or a CF_3 group at the *meta*-position (Table 2, entries 9 and 10), cyclization occurred preferentially at the less hindered position with two separable regioisomeric 3-arylquinolin-2-one products **2i**/**2i′** and **2j**/**2j′** formed in each case. *Ortho*-substituted substrates were also compatible with the methods as demonstrated by the formation of **2k** and **2l** (Table 2, entries 11 and 12). Further investigation was focused on the substituent effect of the acrylic motif of R^3. Entries 13−16 show that reactants containing substituted aryl R^3 groups, regardless of the electronic nature of the substituent, all delivered the corresponding 3-aryl-quinolinones in acceptable yields, though lower in comparison with the unsubstituted counterpart **1a**. It should be mentioned that **2q** is a key intermediate in the construction of naturally occurring cryptotackieine **1** and cryptosanguinolentine **2**.[3e] In addition, we found that the method could be potentially applied to heterocyclic R^3 groups, as illustrated by the transformation of the 2-thienyl-substituted acylic amide, although the yield was a modest 30%. Attempts to extend the method to alkyl-substituted acrylamides was found to be unsuccessful, as the reaction of *N*-methyl-*N*-phenylbut-2-enamide **1s** turned out to be sluggish with no cyclized product detected (Table 2, entry 18).

In order to gain more insights into the reaction, we designed and synthesized a series of 3,3-disubstituted acrylamides with varying properties in the size of the steric hindrance, electronic effects, and configurations. The results are listed in Table 3. Reactions occurred for the 3,3-diarylacrylamides bearing two identical substituents (**3a−c**) in an identical pattern, all affording the desired product **4a−c** in moderate to good yields (Table 3, entries 1−3). Among the three substrates, **3c**, bearing the electron-donating *para*-methoxy substituent, gave the highest yield. In the case of **3d**, where one of the phenyl groups in **3a** was replaced by a less bulky methyl group, the reaction afforded only the phenyl-migrated product in 86% yield, with no detection of the methyl migrated product (Table 3, entry 4). For substrates **3e−h** which contained two aromatic rings of different electron densities in the acrylic moiety, only one single product (**4e−h**) with specifically the aryl group in the *trans*-position having migrated was formed (Table 3, entries 5−8).

DOI: 10.1021/acs.joc.6b00345
J. Org. Chem. 2016, 81, 4058−4065

Table 3. Further Investigation on the PIFA-Mediated C−C Bond Formation and 1,2-Aryl Migration Reaction[a]

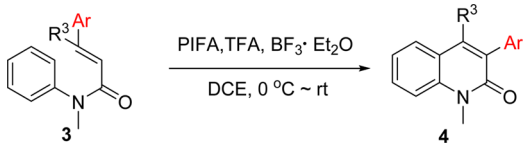

Entry	Substrate	Product[b]	Entry	Substrate	Product[b]
1	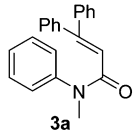 **3a**	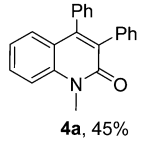 **4a**, 45%	6	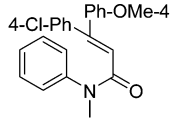 **3f**	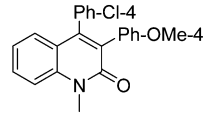 **4f**, 63%
2	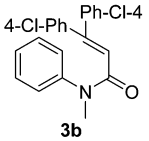 **3b**	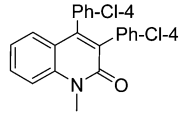 **4b**, 38%	7	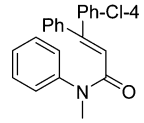 **3g**	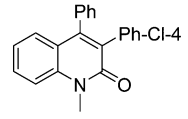 **4g**, 71%
3	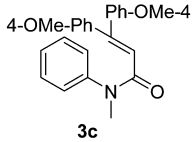 **3c**	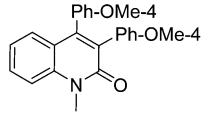 **4c**, 67%	8	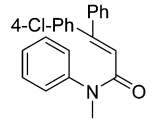 **3h**	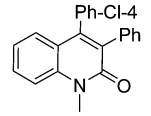 **4h**, 66%
4	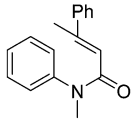 **3d**	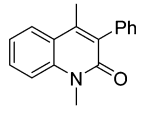 **4d**, 86%	9[c]	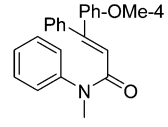 **3i**	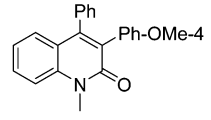 **4i**
5	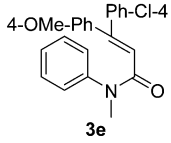 **3e**	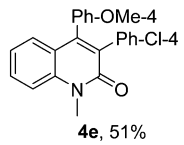 **4e**, 51%		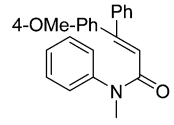 **3i'**	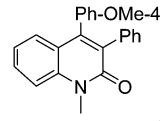 **4i'**, 68%[d]

[a]All reactions were carried out with **3** (0.4 mmol) and PIFA (1.5 equiv) in DCE (16 mL). [b]Isolated yield. [c]The ratio of **3i** and **3i′** is 1.0:0.80, determined by ^{1}H NMR analysis. [d]The ratio of **4i** and **4i′** is 1.0:0.8 by ^{1}H NMR analysis.

For the reaction containing an inseparable mixture of *E* and *Z* geometric isomers **3i** and **3i′**, a mixture of two regioisomeric products **4i** and **4i′** was formed, in a ratio practically identical to that of **3i** and **3i′** (Table 3, entry 9). The results of these examples revealed the regiospecific nature of the reaction mechanism, dominated by the position of the aryl group irrelevant to the electronic effect of the groups.

The newly discovered regiospecific nature of the reaction led us to reconsider the previously proposed mechanism.[11] We show it again here in Scheme 1, path **a**. In this mechanistic pathway, the carbonyl oxygen was proposed to attack the electron-deficient hypervalent iodine(III) reagent, and the 1,2-aryl migration occurred on the tetrahedral C3 in intermediate **III**. Obviously, such a pathway cannot account for the regiospecific character observed in this research.

Herein, we propose a different pathway (Scheme 1, path **b**) in which the alkenyl double bond initiates the nucleophilic attack on the hypervalent iodine(III) reagent. Regioselectivity is controlled through a preferred, unhindered side during the aromatic electrophilic substitution reaction in forming **II′**, as well as an intramolecular S_N2-type of reaction of **III′** during the aryl migration. The X-ray crystallography structure of **3g** supports the proposition, as the molecule is shown to be nonplanar, having the alkenyl moiety twisted out of the plane to form an almost T-shaped arrangement likely to benefit from the extra stability brought by $\pi-\pi$ stacking interactions.

The new mechanism (path **b**) also explains the experimental observation of electron-rich aryl groups favoring the reaction (Table 3, **3a−c**), as intermediate **I′** is a benzylic carbocation connected to an aryl group, while there is no such intermediate in the mechanism described in path **a**.

In order to acquire more mechanistic details at the atomic level, DFT calculations were carried out on a representative substrate **3g**, as well as all the transition states and intermediates along the reaction pathway. The optimized geometry of **3g** adopts the conformation consistent with its X-ray crystal structure, in which Ph1 blocks one side of the double bond. The reaction initiated with the addition of the electron-deficient hypervalent iodine(III) complex to the carbonyl oxygen of the amide moiety in the substrate, which affords 3-azatriene intermediate **A**, concomitant with release of one trifluoroacetate anion ($CF_3CO_2^-$). Notably, boron trifluoride (BF_3) also participates in this reaction as an important additive to stabilize the leaving group, the trifluoroacetate anion ($CF_3CO_2^-$) in the form of a $[CF_3CO_2\cdots BF_3]^-$ anion. Intermediate **A** isomerizes to two enantiomeric intermediates **B** or **B′** via iodonium migration from the carbonyl oxygen to the α-position of the substrate. As the iodonium group in **B** has

DOI: 10.1021/acs.joc.6b00345
J. Org. Chem. 2016, 81, 4058−4065

Scheme 1. Proposed Mechanistic Pathways for the Transformation

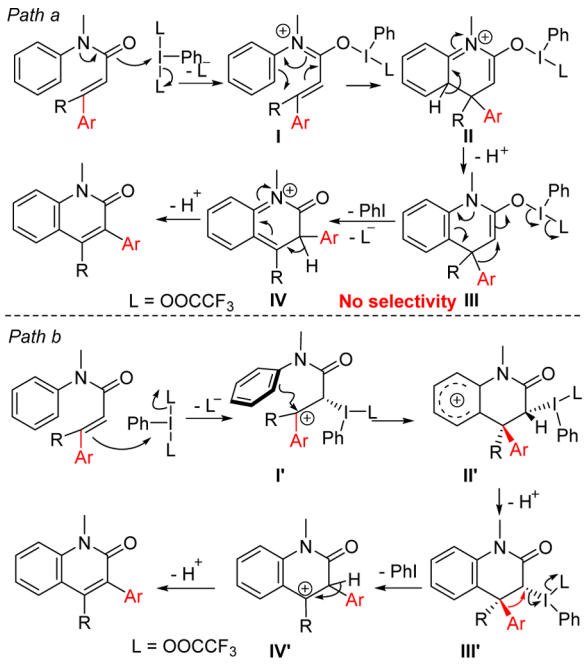

the advantage of a more spacious environment than that in **B′**, it was computed to be 6.1 kcal/mol lower in free energy than **B′**. The transition states **TS-BC** and **TS-BC′** for the ring closure step from **B** and **B′**, respectively, were calculated to have a noticeable free energy difference of 5.8 kcal/mol. The optimized transition-state structures **TS-BC** and **TS-BC′** are illustrated in Figure 2. In **TS-BC** where the iodonium group is *anti*- to the C−C bond being formed, the late transition state occurs with the C−C distance being 1.91 Å. With the bulky iodonium group in close proximity to the forming C−C bond, the Cα−Cβ bond in **TS-BC′** was twisted, while the newly formed C−C bond remains apart with a distance of 2.11 Å. The weaker interaction in **TS-BC′** accounts for its instability.

Consequently, intermediate **C**, resulting from **TS-BC**, in which the iodonium located *trans* to Ph2, was predicted to be the predominant intermediate along the pathway. From **C**, reductive elimination of iodonium(III) releases PhI, giving **D**, in which trifluoroacetate is installed *trans* to the −Ph2. Attempts to locate the transition state for reductive elimination were not successful. Given the significant driving force for the formation of **D**, the process may be barrierless. The −Ph2 at Cβ in **D** could undergo 1,2-aryl-migration with the expulsion of $CF_3CO_2^-$ anion via **TS-DE**. Coordination of Lewis acid, boron trifluoride (BF_3), to the trifluoroacetate anion ($CF_3CO_2^-$) is expected to promote the dissociation of the leaving group. **TS-DE′**, with an activation barrier of 23.7 kcal/mol, was indeed

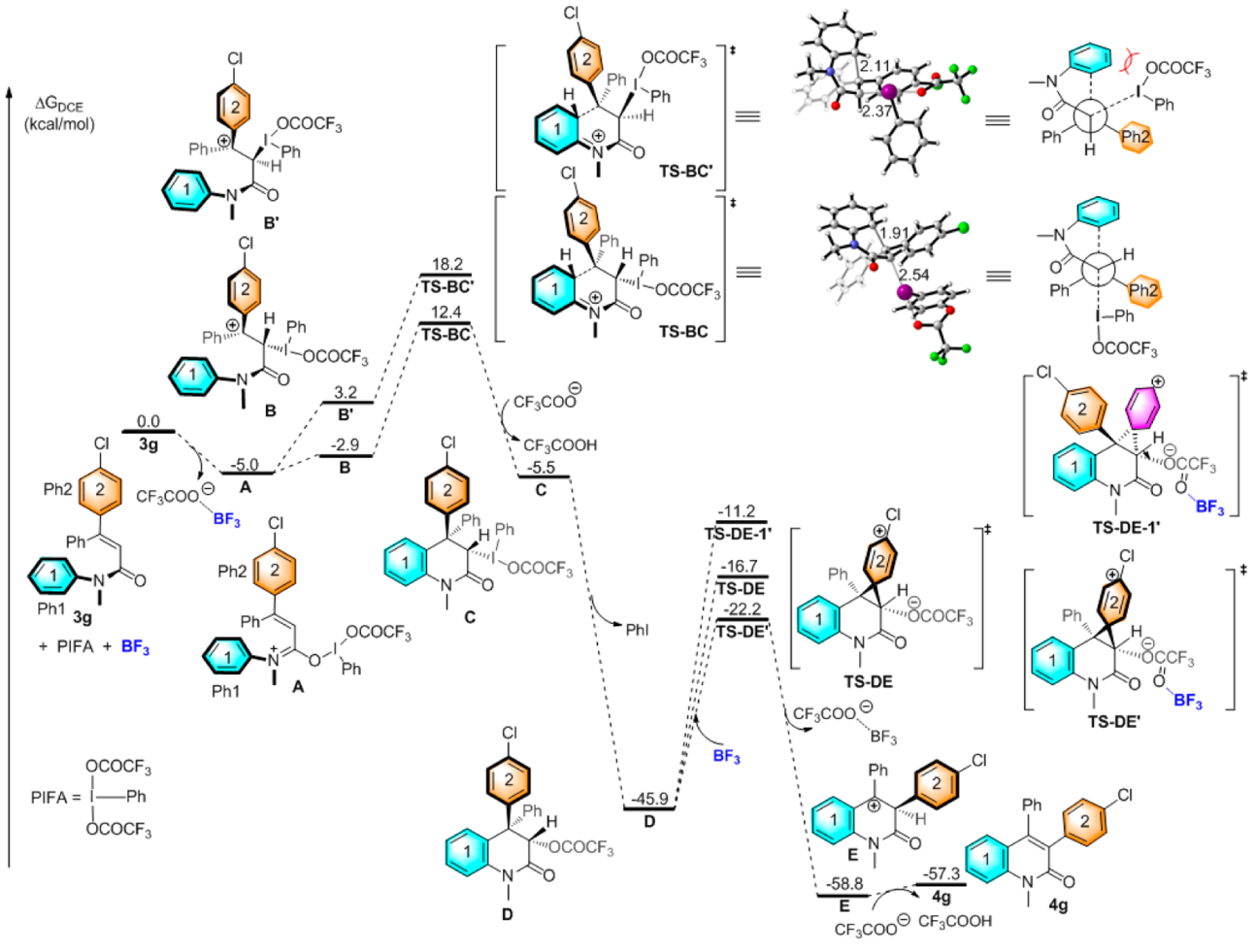

Figure 2. Free energy profile (kcal/mol) of the formation of 3-arylquinolin-2-one in DCE as solvent calculated at M06/6-311++G(d,p).

DOI: 10.1021/acs.joc.6b00345
J. Org. Chem. 2016, 81, 4058−4065

found to be more favorable than **TS-DE**. The transition state **TS-DE′** is a typical transition-state structure in an intramoleular S_N2 reaction, which accounts for the stereospecific nature of the reaction. Alternatively, the 1,2-migration of the *syn*-aryl group with the dissociation of the $[CF_3CO_2\cdots BF_3]^-$ anion at the same side was also considered. The *syn*-attack transition structure **TS-DE-1′** was found to be 11.0 kcal/mol higher in energy than **TS-DE′**. Therefore, the *syn*-aryl migration was excluded. The step from **D** to **E** is exergonic due to the resonance stability in **E**. For this reason, the aryl group is indispensible as we have observed in our experiments (Table 1, entry 18). Additional calculations were carried out for the free energy barrier for the methyl migration, via **TS-DE-methyl**, and this was computed to be 42.5 kcal/mol, a prohibitively high value (see the Supporting Information for calculation details). Facile deprotonation of **E** yields the final product 3-phenylquinolin-2-one (**4g**).

CONCLUSION

In conclusion, we have developed a novel metal-free protocol for the preparation of the quinolin-2-one framework from readily available *N*-arylcinnamic amides. This hypervalent iodine reagent-mediated reaction involves a cascade sequence of oxidative annulation and a highly regioselective 1,2-aryl migration process. A mechanism was proposed which accounts for the high regioselectivity observed experimentally and is supported by the computational results. Further investigations on the scope and application of this method are currently ongoing in our laboratory.

EXPERIMENTAL SECTION

General Information. All reactions were carried out at room temperature and stirred magnetically. ^{1}H and ^{13}C NMR spectra were recorded on a 400 MHz or 600 MHz spectrometer at 25 °C. Chemical shifts values are given in ppm and referred as the internal standard to TMS: 0.00 ppm. The peak patterns are indicated as follows: s, singlet; d, doublet; t, triplet; q, quartet; qui, quintet; m, multiplet, and dd, doublet of doublets. The coupling constants *J*, are reported in hertz (Hz). High-resolution mass spectrometry (HRMS) was obtained on a Q-TOF micro spectrometer. Melting points were determined with a MicroMelting point apparatus without corrections. Organic solutions were concentrated by rotary evaporation below 40 °C in vacuum. TLC plates were visualized by exposure to ultraviolet light. Reagents and solvents were purchased as reagent grade and were used without further purification. All reactions were performed in standard glassware, heated at 70 °C for 3 h before use. Flash column chromatography was performed over silica gel 200−300 m, and the eluent was a mixture of ethyl acetate (EA) and petroleum ether (PE).

Preparation of Substrates 1 and 3.[11] To a suspension of the acid (1.0 equiv) in DCM (0.3 M) was added a catalytic amount of DMF (0.1 mL/mmol acid). At ambient temperature, oxalyl chloride (1.5 equiv) was added dropwise over a period of 0.5 h, forming a homogeneous solution. The resulting solution was kept at room temperature for 3 h. Then, the solvent was removed under reduced pressure. The residue was dissolved in dry DCM and slowly added dropwise to a solution of the appropriate aniline derivative (1.0 equiv) and Et_3N (2.5 equiv) in DCM (0.25 M). The reaction mixture was maintained at ambient temperature and monitored by TLC. Upon completion, the mixture was extracted with CH_2Cl_2 (3× 50 mL), and the combined organic phase was washed with aq saturated NH_4Cl (1 × 80 mL) and saturated brine (1 × 80 mL), then dried over Na_2SO_4. Evaporation of the solvent under reduced pressure and purification of the crude residue by flash column chromatography on silica gel (EA/PE) afforded the desired amides.

Compounds **1a−s** and **3a−c** have been reported in our previous work.[11] The new compounds thus obtained were characterized as follows:

*(E)-N-Methyl-N,3-diphenylbut-2-enamide (**3d**).* Following the general procedure, **3d** was purified by silica gel chromatography (15% EA/PE) to give a yellow oil, 355 mg, yield: 55%. ^{1}H NMR (600 MHz, $CDCl_3$) δ 7.36 (t, *J* = 8.0 Hz, 2H), 7.26 (t, *J* = 7.5 Hz, 1H), 7.24−7.11 (m, 7H), 5.96 (s, 1H), 3.37 (s, 3H), 2.50 (s, 3H). ^{13}C NMR (150 MHz, $CDCl_3$) δ 167.3, 148.8, 144.1, 142.7, 129.4, 128.3, 128.2, 127.3, 126.9, 126.1, 119.8, 37.0, 18.0. HRMS (ESI) *m*/*z* calcd for $C_{17}H_{18}NO$ $[M + H^+]$ 252.1388, found 252.1385.

*(E)-3-(4-Chlorophenyl)-3-(4-methoxyphenyl)-N-methyl-N-phenylacrylamide (**3e**).* Following the general procedure, **3e** was purified by silica gel chromatography (15% EA/PE) to give a pale oil, 353 mg, yield: 33%. ^{1}H NMR (600 MHz, $CDCl_3$) δ 7.33−7.27 (m, 4H), 7.21 (t, *J* = 7.4 Hz, 1H), 7.04 (d, *J* = 7.3 Hz, 2H), 6.98 (d, *J* = 7.5 Hz, 2H), 6.93 (d, *J* = 7.6 Hz, 2H), 6.74 (d, *J* = 8.2 Hz, 2H), 6.11 (s, 1H), 3.76 (s, 3H), 3.24 (s, 3H). ^{13}C NMR (150 MHz, $CDCl_3$) δ 167.1, 160.1, 148.1, 143.6, 137.9, 133.9, 133.5, 130.9, 129.4, 129.1, 128.1, 127.0, 126.6, 119.7, 113.6, 55.3, 36.8. HRMS (ESI) *m*/*z* calcd for $C_{23}H_{21}{}^{35}ClNO_2^+$ $[M + H^+]$ 378.1261, found 378.1263.

*(Z)-3-(4-Chlorophenyl)-3-(4-methoxyphenyl)-N-methyl-N-phenylacrylamide (**3f**).* Following the general procedure, **3f** was purified by silica gel chromatography (10% EA/PE) to afford a white solid, 351.0 mg, yield: 31%, mp 133−135 °C. ^{1}H NMR (600 MHz, $CDCl_3$) δ 7.24 (d, *J* = 7.2 Hz, 2H), 7.18 (d, *J* = 7.6 Hz, 3H), 6.97 (d, *J* = 7.8 Hz, 2H), 6.94 (d, *J* = 7.9 Hz, 2H), 6.90−6.80 (m, 4H), 6.04 (s, 1H), 3.85 (s, 3H), 3.24 (s, 3H). ^{13}C NMR (150 MHz, $CDCl_3$) δ 167.7, 159.8, 147.0, 143.8, 140.4, 134.3, 131.0, 131.0, 129.5, 128.9, 128.3, 126.9, 126.5, 121.1, 113.3, 55.3, 36.6. HRMS (ESI) *m*/*z* calcd for $C_{23}H_{20}{}^{35}ClNNaO_2^+$ $[M + H^+]$ 400.1080, found 400.1084.

*(E)-3-(4-Chlorophenyl)-N-methyl-N,3-diphenylacrylamide (**3g**).* Following the general procedure, **3g** was purified by silica gel chromatography (10% EA/PE) to give a pale yellow solid, 468.5 mg, yield: 45%, mp 107−109 °C. ^{1}H NMR (600 MHz, $CDCl_3$) δ 7.36−7.30 (m, 3H), 7.26−7.22 (m, 2H), 7.19 (t, *J* = 8.0 Hz, 3H), 7.03 (d, *J* = 7.0 Hz, 2H), 6.94 (d, *J* = 8.0 Hz, 2H), 6.85 (d, *J* = 7.5 Hz, 2H), 6.14 (s, 1H), 3.22 (s, 3H). ^{13}C NMR (150 MHz, $CDCl_3$) δ 167.3, 147.2, 143.5, 140.0, 138.6, 134.4, 129.5, 129.4, 128.9, 128.4, 127.9, 126.9, 126.5, 121.9, 36.6 (two carbon peaks overlapped). HRMS (ESI) *m*/*z* calcd for $C_{22}H_{19}{}^{35}ClNO$ $[M + H^+]$ 348.1155, found 348.1153.

*(Z)-3-(4-Chlorophenyl)-N-methyl-N,3-diphenylacrylamide (**3h**).* Following the general procedure, **3h** was purified by silica gel chromatography (10% EA/PE) to give a yellow oil, 323.4 mg, yield: 45%. ^{1}H NMR (600 MHz, $CDCl_3$) δ 7.34−7.27 (m, 4H), 7.26−7.24 (m, 1H), 7.23−7.19 (m, 3H), 7.03 (d, *J* = 8.0 Hz, 2H), 6.98 (d, *J* = 7.0 Hz, 2H), 6.94 (d, *J* = 7.5 Hz, 2H), 6.18 (s, 1H), 3.25 (s, 3H). ^{13}C NMR (150 MHz, $CDCl_3$) δ 167.1, 147.7, 143.5, 141.2, 137.6, 134.1, 131.0, 129.1, 128.6, 128.3, 128.1, 128.0, 127.0, 126.5, 121.8, 36.7. HRMS (ESI) *m*/*z* calcd for $C_{22}H_{19}{}^{35}ClNO$ $[M + H^+]$ 348.1155, found 348.1153.

*3-(4-Methoxyphenyl)-N-methyl-N,3-diphenylacrylamide (**3i**).* Following the general procedure, **3i** was purified by silica gel chromatography (15% EA/PE) and isolated as a mixture of the *E*/*Z* isomers, yellow oil, 556.3 mg, yield: 55%, *E*/*Z* ratio is 1:0.8. ^{1}H NMR (600 MHz, $CDCl_3$) Major isomer (*E*) δ 7.37−7.30 (m, 3H, peaks of two isomers overlapped), 7.25−7.18 (m, 8H, peaks of two isomers overlapped), 7.0−6.95 (m, 5H, peaks of two isomers overlapped), 6.93−6.87 (m, 4H, peaks of two isomers overlapped), 6.86−6.81 (m, 2H), 6.08 (s, 1H), 3.84 (s, 3H), 3.24 (s, 3H); Minor isomer (*Z*) δ 7.37−7.30 (m, 3H, peaks of two isomers overlapped), 7.25−7.18 (m, 8H, peaks of two isomers overlapped), 7.10−7.04 (m, 2H), 6.93−6.87 (m, 4H, peaks of two isomers overlapped),6.77−6.69 (m, 2H), 6.11 (s, 1H), 3.76 (s, 3H), 3.21 (s, 3H). ^{13}C NMR (150 MHz, $CDCl_3$) Major isomer δ167.7, 159.9, 143.8, 139.4, 134.0, 131.1, 129.6, 129.4, 128.9, 128.3, 128.0, 126.7, 126.6, 119.7, 113.6, 55.3, 36.7. Minor isomer 168.0,159.7,148.7, 148.3,143.7, 131.5,129.2, 128.8, 128.3,128.1, 127.8, 126.7,120.8,113.2, 112.8, 36.6 (one carbon peak missed due to overlapped). HRMS (ESI) *m*/*z* calcd for $C_{23}H_{22}NO_2$ $[M + H^+]$ 344.1651, found 344.1649. The ratio of the two isomers was determined by NMR in DMSO-d_6. *E*/*Z* ratio is 1.0:0.8. ^{1}H NMR (600 MHz, DMSO-d_6) Major isomer (*E*) δ 7.36−7.25 (m, 11H, peaks of two isomers overlapped), 7.23−7.16 (m, 2H, peaks of two isomers

DOI: 10.1021/acs.joc.6b00345
J. Org. Chem. 2016, 81, 4058−4065

overlapped), 7.10−7.02 (m, 4H, peaks of two isomers overlapped), 7.01−6.80 (m, 10H, peaks of two isomers overlapped), 6.09 (s, 1H), 3.79 (s, 3H), 3.13 (s, 3H); Minor isomer (*Z*) δ 7.36−7.25 (m, 11H, peaks of two isomers overlapped), 7.23−7.16 (m, 2H, peaks of two isomers overlapped), 7.10−7.02 (m, 4H, peaks of two isomers overlapped), 7.01−6.80 (m, 10H, peaks of two isomers overlapped), 6.12 (s, 1H), 3.72 (s, 3H), 3.11 (s, 3H).

Preparation of Quinolinones 2 and 4. *General Procedure.* To a solution of substrate **1** or **3** (0.4 mmol) in DCE (16 mL) was slowly added TFA (10 equiv) at 0 °C. Then, a solution of PIFA (1.5 equiv) and $BF_3{\cdot}Et_2O$ (1.0 equiv) in DCE (2.5 mL) was added dropwise to the mixture with stirring. The resulting mixture was maintained at room temperature, and the progress of the reaction was monitored by TLC. Upon completion, the reaction mixture was poured into cold water (30 mL) and extracted with CH_2Cl_2 (3 × 30 mL). The combined organic layer was washed with saturated $NaHCO_3$ (1 × 60 mL) and brine (1 × 60 mL) before being dried over Na_2SO_4. The solvent was removed under vacuum, and the residue was purified by silica gel chromatography, using a mixture of PE/EA to afford the desired product **2** or **4**.

Compounds **2a−r** and **4a−c** have been reported in our previous work.[11] The new compounds thus obtained were characterized as follows:

*1,4-Dimethyl-3-phenylquinolin-2(1H)-one (**4d**).*[24] Following the general procedure, **4d** was purified by silica gel chromatography (10% EA/PE) to give a yellow solid, 85.7 mg, yield: 86%, mp 135−136 °C. ^{1}H NMR (600 MHz, $CDCl_3$) δ 7.81 (dd, *J* = 8.0, 1.0 Hz, 1H), 7.59 (t, *J* = 8.0 Hz, 1H), 7.47−7.39 (m, 3H), 7.37 (d, *J* = 7.5 Hz, 1H), 7.30−7.26 (m, 3H), 3.77 (s, 3H), 2.33 (s, 3H). HRMS (ESI) *m*/*z* calcd for $C_{17}H_{16}NO^+$ [M + H$^+$] 250.1232, found 250.1228.

*3-(4-Chlorophenyl)-4-(4-methoxyphenyl)-1-methylquinolin-2(1H)-one (**4e**).*[25] Following the general procedure, **3e** was purified by silica gel chromatography (10% EA/PE) to give a yellow solid, 76.5 mg, yield: 51%, mp 194−195 °C. ^{1}H NMR (600 MHz, $CDCl_3$) δ 7.58 (t, *J* = 7.4 Hz, 1H), 7.44 (d, *J* = 8.4 Hz, 1H), 7.36 (d, *J* = 7.8 Hz, 1H), 7.18−7.11 (m, 3H), 7.04 (d, *J* = 8.3 Hz, 2H), 7.00 (d, *J* = 8.5 Hz, 2H), 6.82 (d, *J* = 8.5 Hz, 2H), 3.83 (s, 3H), 3.80 (s, 3H). ^{13}C NMR (150 MHz, $CDCl_3$) δ 161.6, 159.0, 147.8, 139.6, 134.7, 132.7, 132.1, 131.1, 130.9, 130.5, 128.6, 128.2, 127.8, 122.0, 121.7, 114.1, 113.6, 55.2, 30.1. HRMS (ESI) *m*/*z* calcd for $C_{23}H_{19}{}^{35}ClNO_2^+$ [M + H$^+$] 376.1104, found 376.1101.

*4-(4-Chlorophenyl)-3-(4-methoxyphenyl)-1-methylquinolin-2(1H)-one (**4f**).* Following the general procedure, **4f** was purified by silica gel chromatography (15% EA/PE) to give a pale solid, 94.5 mg, yield: 63%, mp 195−196 °C. ^{1}H NMR (600 MHz, $CDCl_3$) δ 7.60−7.55 (m, 1H), 7.45 (d, *J* = 8.4 Hz, 1H), 7.29−7.23 (m, 3H), 7.13 (t, *J* = 7.6 Hz, 1H), 7.05 (d, *J* = 8.4 Hz, 2H), 7.03−6.99 (m, 2H), 6.73 (d, *J* = 8.7 Hz, 2H), 3.84 (s, 3H), 3.75 (s, 3H). ^{13}C NMR (150 MHz, $CDCl_3$) δ 161.9, 158.5, 146.2, 139.5, 135.1, 133.5, 131.9, 131.8, 131.3, 130.3, 128. 1, 128.0, 127.8, 122.0, 121.3, 114.2, 113.2, 55.1, 30.2. HRMS (ESI) *m*/*z* calcd for $C_{23}H_{19}{}^{35}ClNO_2^+$ [M + H$^+$] 376.1104, found 376.1103.

*3-(4-Chlorophenyl)-1-methyl-4-phenylquinolin-2(1H)-one (**4g**).*[25] Following the general procedure, **4g** was purified by silica gel chromatography (15% EA/PE) to give a yellowish solid, 98.0 mg, yield: 71%, mp 205−207 °C. ^{1}H NMR (600 MHz, $CDCl_3$) δ 7.58 (t, *J* = 8.0 Hz, 1H), 7.45 (d, *J* = 8.5 Hz, 1H), 7.32−7.27 (m, 4H), 7.15−7.11 (m, 3H), 7.09 (dd, *J* = 7.5, 2.0 Hz, 2H), 7.04 (d, *J* = 8.5 Hz, 2H), 3.84 (s, 3H). ^{13}C NMR (150 MHz, $CDCl_3$) δ 161.6, 148.0, 139.6, 136.1, 134.5, 132.8, 132.1, 130.8, 130.8, 129.8, 128.6, 128.2, 127.8, 127.7, 122.0, 121.4, 114.1, 30.2. HRMS (ESI) *m*/*z* calcd for $C_{22}H_{17}{}^{35}ClNO^+$ [M + H$^+$] 346.0999, found 346.0995.

*4-(4-Chlorophenyl)-1-methyl-3-phenylquinolin-2(1H)-one (**4h**).* Following the general procedure, **4h** was purified by silica gel chromatography (15% EA/PE) to give a pale yellow solid, 91.1 mg, yield: 66%, mp. 203−205 °C. ^{1}H NMR (600 MHz, $CDCl_3$) δ 7.58 (ddd, *J* = 8.5, 7.0, 1.5 Hz, 1H), 7.45 (d, *J* = 8.0 Hz, 1H), 7.28−7.23 (m, 3H), 7.21−7.17 (m, 2H), 7.17−7.11 (m, 2H), 7.10−7.07 (m, 2H), 7.06−7.03 (m, 2H), 3.84 (s, 3H). ^{13}C NMR (150 MHz, $CDCl_3$) δ 161.7, 146.4, 139.6, 135.7, 134.9, 133.6, 132.4, 131.3, 130.5, 130.5, 128.3, 128.2, 127.7, 127.1, 122.0, 121.2, 114.2, 30.2. HRMS (ESI) *m*/*z* calcd for $C_{22}H_{17}{}^{35}ClNO^+$ [M + H$^+$] 346.0999, found 346.0997.

*3-(4-Methoxyphenyl)-1-methyl-4-phenylquinolin-2(1H)-one (**4i**).*[25] Following the general procedure, **4i** was purified by silica gel chromatography (15% EA/PE) to give a yellow solid, 50.5 mg, yield 37%, mp 167−169 °C. ^{1}H NMR (600 MHz, $CDCl_3$) δ 7.58−7.52 (m, 1H), 7.43 (d, *J* = 8.5 Hz, 1H), 7.29−7.25 (m, 4H), 7.11 (dt, *J* = 7.0, 2.0 Hz, 3H), 7.03 (dd, *J* = 8.5, 1.5 Hz, 2H), 6.70 (d, *J* = 8.0 Hz, 2H), 3.84 (s, 3H), 3.72 (s, 3H). ^{13}C NMR (150 MHz, $CDCl_3$) δ 158.4, 147.5, 139.5, 136.6, 131.9, 130.1, 129.9, 128.4, 128.3, 128.2, 128.0, 127.5, 127.4, 121.9, 121.6, 114.0, 113.0, 55.1, 30.2. HRMS (ESI) *m*/*z* calcd for $C_{23}H_{20}NO_2^+$ [M + H$^+$] 342.1494, found 342.1488.

*4-(4-Methoxyphenyl)-1-methyl-3-phenylquinolin-2(1H)-one (**4i′**).* Following the general procedure, **4i′** was purified by silica gel chromatography (15% EA/PE) to give a pale solid, 42.3 mg, yield 31%, mp 159−161 °C. ^{1}H NMR (600 MHz, $CDCl_3$) δ 7.56 (ddd, *J* = 8.5, 7.0, 1.5 Hz, 1H), 7.44 (d, *J* = 8.0 Hz, 1H), 7.36 (dd, *J* = 8.0, 1.5 Hz, 1H), 7.19−7.16 (m, 2H), 7.15−7.08 (m, 4H), 7.04−6.99 (m, 2H), 6.81−6.77 (m, 2H), 3.84 (s, 3H), 3.77 (s, 3H). ^{13}C NMR (151 MHz, $CDCl_3$) δ 161.9, 158.9, 147.5, 139.6, 136.2, 132.2, 131.2, 130.7, 130.2, 128.6, 128.5, 127.5, 126.8, 121.8, 114.0, 113.5, 55.2, 30.1 (two carbon peaks overlapped). HRMS (ESI) *m*/*z* calcd for $C_{23}H_{20}NO_2^+$ [M + H$^+$] 342.1494, found 342.1490.

Computational Details. DFT calculations were performed with the Gaussian 09 suite of programs.[14] Reactants, transition states (TSs), intermediates, and products were optimized at the hybrid density functional B3LYP[15] level of theory with basis set I (BSI):LANL2DZ[16] incorporating a relativistic pseudopotential (effective core potential, ECP)[17] for I and 6-31G(d)[18] basis set for the rest of the elements. Single point energy calculations were then conducted at the M06[19] level of theory with basis set II (BSII): Stuttgart-Dresden basis set (SDD)[20] incorporating ECP for I and 6-311++G(d,p) for other elements. The SMD solvent model with the parameters for dichloroethane (DCE) were employed to account for solvent effects.[21]

All vibrational frequencies were computed at the B3LYP/BSI to verify the stationary points and provide the thermal corrections. Intrinsic reaction coordinate (IRC)[22] analyses were performed to confirm that a specific TS connects the two relevant minima. All energies presented are Gibbs free energies at 298 K in DCE in kcal/mol unless otherwise stated. Geometries were illustrated using CYLVIEW drawings.[23]

■ ASSOCIATED CONTENT

Supporting Information

The Supporting Information is available free of charge on the ACS Publications website at DOI: 10.1021/acs.joc.6b00345.

Crystallographic data for **3g** (CIF)
Crystallographic data for **4g** (CIF)
Spectral data for all new compounds, X-ray structures and data of **3g** and **4g**, and computational data (PDF)

■ AUTHOR INFORMATION

Corresponding Authors

*E-mail: duyunfeier@tju.edu.cn (Y.D.).
*E-mail: wuyd@pkusz.edu.cn (Y.-D.W.).
*E-mail: kangzhao@tju.edu.cn (K.Z.).

Author Contributions

§These authors contributed equally to the work.

Notes

The authors declare no competing financial interest.

■ ACKNOWLEDGMENTS

We acknowledge the National Natural Science Foundation of China (#21072148, #21133002, #21302006), the Tianjin Research Program of Application Foundation and Advanced Technology (#15JCZDJC32900), and the National Basic

DOI: 10.1021/acs.joc.6b00345
J. Org. Chem. 2016, 81, 4058−4065

Research Project (2014CB932201, 2013CB911501) for financial support.

REFERENCES

(1) For selected examples, see: (a) Godula, K.; Sames, D. *Science* **2006**, *312*, 67. (b) Lyons, T. W.; Sanford, M. S. *Chem. Rev.* **2010**, *110*, 1147. (c) Tang, S.; Liu, K.; Liu, C.; Lei, A. *Chem. Soc. Rev.* **2015**, *44*, 1070. (d) Huang, H.; Ji, X.; Wu, W.; Jiang, H. *Chem. Soc. Rev.* **2015**, *44*, 1155. (e) Topczewski, J. J.; Sanford, M. S. *Chem. Sci.* **2015**, *6*, 70. (f) Guo, X.; Gu, D.; Wu, Z.; Zhang, W. *Chem. Rev.* **2015**, *115*, 1622. (g) Kuhl, N.; Hopkinson, M. N.; Wencel-Delord, J.; Glorius, F. *Angew. Chem., Int. Ed.* **2012**, *51*, 10236.

(2) For selected examples, see: (a) Tsang, W. C. P.; Zheng, N.; Buchwald, S. L. *J. Am. Chem. Soc.* **2005**, *127*, 14560. (b) Hennessy, E.; Bulchwald, S. L. *J. Am. Chem. Soc.* **2003**, *125*, 12084. (c) Maehara, A.; Tsurugi, H.; Satoh, T.; Miura, M. *Org. Lett.* **2008**, *10*, 1159. (d) Pastine, S. J.; McQuaid, K. M.; Sames, D. *J. Am. Chem. Soc.* **2005**, *127*, 12180. (e) Bernini, R.; Fabrizi, G.; Sferrazza, A.; Cacchi, S. *Angew. Chem., Int. Ed.* **2009**, *48*, 8078.

(3) (a) Chen, I.; Tsai, I.; Teng, C.; Chen, J.; Chang, Y.; Ko, F.; Lu, M.; Pezzuto, J. *Phytochemistry* **1997**, *46*, 525. (b) Ferrer, P.; Avendano, C.; Sollhuber, M. *Liebigs Ann.* **1995**, *1995*, 1895. (c) Okuzumi, T.; Yoshimura, T.; Nakanishi, E.; Ono, M.; Murata, M. Novel Phenylalanine Derivatives. WO 03/053926 A1, July 3, 2003. (d) Bair, K. W.; Lancia, D. R.; Li, H.; Loch, J.; Lu, L.; Martin, M. W.; Millan, D.; Scheller, S.; Tebbe, M. J. Novel compounds and compositions for inhibition of FASN. WO 2014/144749 A1, March11, 2014. (e) Fresneda, P. M.; Molina, P.; Delgado, S. *Tetrahedron* **2001**, *57*, 6197.

(4) (a) Joseph, B.; Darro, F.; Behard, A.; Lesur, B.; Collignon, F.; Decaestecker, C.; Frydman, A.; Guillaumet, G.; Kiss, R. *J. Med. Chem.* **2002**, *45*, 2543. (b) Huang, L.; Hsieh, M.; Teng, C.; Lee, K.; Kuo, S. *Bioorg. Med. Chem.* **1998**, *6*, 1657. (c) Anzini, M.; Cappelli, A.; Vomero, S.; Giorgi, G.; Langer, T.; Hamon, M.; Merahi, N.; Emerit, B. M.; Cagnotto, A.; Skorupska, M.; Mennini, T.; Pinto, J. C. *J. Med. Chem.* **1995**, *38*, 2692.

(5) For selected examples, see: (a) Manske, R. H. *Chem. Rev.* **1942**, *30*, 113. (b) Wu, J.; Xia, H.; Gao, K. *Org. Biomol. Chem.* **2006**, *4*, 126. (c) Jia, C.; Zhang, Z.; Tu, S.; Wang, G. *Org. Biomol. Chem.* **2006**, *4*, 104.

(6) For selected examples, see: (a) Kulkarni, B. A.; Ganesan, A. *Chem. Commun.* **1998**, 785. (b) Liu, X.; Xin, X.; Xiang, D.; Zhang, R.; Kumar, S.; Zhou, F.; Dong, D. *Org. Biomol. Chem.* **2012**, *10*, 5643.

(7) For selected examples, see: (a) Shibuya, T.; Shibata, Y.; Noguchi, K.; Tanaka, K. *Angew. Chem., Int. Ed.* **2011**, *50*, 3963. (b) Kadnikov, D.; Larock, R. C. *J. Org. Chem.* **2004**, *69*, 6772. (c) Iwai, T.; Fujihara, T.; Terao, J.; Tsuji, Y. *J. Am. Chem. Soc.* **2010**, *132*, 9602. (d) Mai, W.; Sun, G.; Wang, J.; Song, G.; Mao, P.; Yang, L.; Yuan, J.; Xiao, Y.; Qu, L. *J. Org. Chem.* **2014**, *79*, 8094. (e) Li, X.; Li, X.; Jiao, N. *J. Am. Chem. Soc.* **2015**, *137*, 9246. (f) Zeng, R.; Dong, G. *J. Am. Chem. Soc.* **2015**, *137*, 1408.

(8) For selected examples, see: (a) Samanta, R.; Matcha, K.; Antonchick, A. P. *Eur. J. Org. Chem.* **2013**, *2013*, 5769. (b) Bering, L.; Antonchick, A. P. *Org. Lett.* **2015**, *17*, 3134. (c) Liu, X.; Meng, Z.; Li, C.; Lou, H.; Liu, L. *Angew. Chem., Int. Ed.* **2015**, *54*, 6012. (d) Wang, X.; Gallardo-Donaire, G.; Martin, R. *Angew. Chem., Int. Ed.* **2014**, *53*, 11084. (e) Narayan, R.; Antonchick, A. P. *Chem.—Eur. J.* **2014**, *20*, 4568. (f) Shen, T.; Yuan, Y.; Jiao, N. *Chem. Commun.* **2014**, *50*, 554.

(9) For selected examples, see: (a) Zhdankin, V. V.; Stang, P. J. *Chem. Rev.* **2008**, *108*, 5299. (b) Wirth, T. *Angew. Chem., Int. Ed.* **2005**, *44*, 3656. (c) Richardson, R. D.; Wirth, T. *Angew. Chem., Int. Ed.* **2006**, *45*, 4402. (d) Dohi, T.; Kita, Y. *Chem. Commun.* **2009**, *16*, 2073. (e) Zhdankin, V. V. *Hypervalent Iodine Chemistry*; Wiley: Chichester, U.K., 2014. (f) Zheng, Z.; Zhang-Negrerie, D.; Du, Y.; Zhao, K. *Sci. China: Chem.* **2014**, *57*, 189. (g) Samanta, R.; Matcha, K.; Antonchick, A. P. *Eur. J. Org. Chem.* **2013**, *2013*, 5769.

(10) For selected examples of our previous work on hypervalent iodine chemistry, see: (a) Shang, S.; Zhang-Negrerie, D.; Du, Y.; Zhao, K. *Angew. Chem., Int. Ed.* **2014**, *53*, 6216. (b) Wang, J.; Yuan, Y.; Xiong, R.; Zhang-Negrerie, D.; Du, Y.; Zhao, K. *Org. Lett.* **2012**, *14*, 2210. (c) Liu, X.; Cheng, R.; Zhao, F.; Zhang-Negrerie, D.; Du, Y.; Zhao, K. *Org. Lett.* **2012**, *14*, 5480. (d) Liu, L.; Zhang-Negrerie, D.; Du, Y.; Zhao, K. *Org. Lett.* **2014**, *16*, 436. (e) Zheng, Y.; Li, X.; Ren, C.; Zhang-Negrerie, D.; Du, Y.; Zhao, K. *J. Org. Chem.* **2012**, *77*, 10353. (f) Sun, T.-Y.; Wang, X.; Geng, H.; Xie, Y.; Wu, Y.-D.; Zhang, X.; Schaefer, H. F., III *Chem. Commun.* **2016**, *52*, 5371.

(11) Liu, L.; Lu, H.; Wang, H.; Yang, C.; Zhang, X.; Zhang-Negrerie, D.; Du, Y.; Zhao, K. *Org. Lett.* **2013**, *15*, 2906.

(12) For selected examples of hypervalent iodine reagent mediated aryl migration reactions, see: (a) Moriarty, R. M.; Khosrowshahi, J. S.; Prakash, O. *Tetrahedron Lett.* **1985**, *26*, 2961. (b) Boye, A. C.; Meyer, D.; Ingison, C. K.; French, A. N.; Wirth, T. *Org. Lett.* **2003**, *5*, 2157. (c) Singh, F. V.; Rehbein, J.; Wirth, T. *ChemistryOpen* **2012**, *1*, 245. (d) Farid, U.; Malmedy, F.; Claveau, R.; Albers, L.; Wirth, T. *Angew. Chem., Int. Ed.* **2013**, *52*, 7018. (e) Purohit, V.; Allwein, S. P.; Bakale, R. P. *Org. Lett.* **2013**, *15*, 1650. (f) Liu, L.; Du, L.; Zhang-Negrerie, D.; Du, Y.; Zhao, K. *Org. Lett.* **2014**, *16*, 5772. (g) Liu, L.; Zhang-Negrerie, D.; Du, Y.; Zhao, K. *Synthesis* **2015**, *47*, 2924.

(13) For selected examples, see: (a) Tanaka, K.; Kakinoki, O.; Toda, F. *J. Chem. Soc., Chem. Commun.* **1992**, 1053. (b) Ayitou, A. J.; Ugrinov, A.; Sivaguru. *J. Photochem. Photobiol. Sci.* **2009**, *8*, 751. (c) Wu, T.; Mu, X.; Liu, G. *Angew. Chem., Int. Ed.* **2011**, *50*, 12578. (d) Jaegli, S.; Dufour, J.; Wei, H.; Piou, T.; Duan, X.; Vors, J.; Neuville, L.; Zhu, J. *Org. Lett.* **2010**, *12*, 4498. (e) Ueda, S.; Okada, T.; Nagasawa, H. *Chem. Commun.* **2010**, *46*, 2462.

(14) Frisch, M. J.; et al.*Gaussian 09*, revision A.02; Gaussian, Inc.: Wallingford, CT, 2009.

(15) Becke, A. D. *J. Chem. Phys.* **1993**, *98*, 5648.

(16) Hay, P. J.; Wadt, W. R. *J. Chem. Phys.* **1985**, *82*, 299.

(17) (a) Andrae, D.; Häußermann, U.; Dolg, M.; Stoll, H.; Preuß, H. *Theor. Chim. Acta* **1990**, *77*, 123. (b) Weigend, F.; Ahlrichs, R. *Phys. Chem. Chem. Phys.* **2005**, *7*, 3297.

(18) (a) Hehre, W. J.; Ditchfield, R.; Pople, J. A. *J. Chem. Phys.* **1972**, *56*, 2257. (b) Dill, J. D.; Pople, J. A. *J. Chem. Phys.* **1975**, *62*, 2921. (c) Francl, M. M.; Pietro, W. J.; Hehre, W. J.; Binkley, J. S.; Gordon, M. S.; DeFrees, D. J.; Pople, J. A. *J. Chem. Phys.* **1982**, *77*, 3654.

(19) Zhao, Y.; Truhlar, D. G. *Theor. Chem. Acc.* **2008**, *120*, 215.

(20) Bergner, A.; Dolg, M.; Küchle, W.; Stoll, H.; Preuss, H. *Mol. Phys.* **1993**, *80*, 1431.

(21) Marenich, A. V.; Cramer, C. J.; Truhlar, D. G. *J. Phys. Chem. B* **2009**, *113*, 6378.

(22) (a) Fukui, K. *Acc. Chem. Res.* **1981**, *14*, 363. (b) Fukui, K. *J. Phys. Chem.* **1970**, *74*, 4161.

(23) Legault, C. Y. *CYLView*, version 1.0b; Universitéde Sherbrooke: Sherbrooke, Québec, Canada, 2009. http://www.cylview.org.

(24) Iwai, T.; Fujihara, T.; Terao, J.; Tsuji, Y. *J. Am. Chem. Soc.* **2010**, *132*, 9602.

(25) Carrer, A.; Brion, J.; Messaoudi, S.; Alami, M. *Adv. Synth. Catal.* **2013**, *355*, 2044.

DOI: 10.1021/acs.joc.6b00345
J. Org. Chem. 2016, 81, 4058−4065